THE METEOROLOGY OF THE JOVIAN ATMOSPHERE

P. H. STONE
Massachusetts Institute of Technology

The only direct observational evidence available concerning the motions in the Jovian atmosphere are remote measurements of apparent zonal motions. The rapid rotation of the planet makes it likely that these motions are in geostrophic balance and satisfy the thermal wind relation. These relations enable one to deduce from the observed latitudinal variation of zonal velocities that the zones are regions of higher temperatures, anti-cyclonic vorticity, rising motions and enhanced cloudiness, while the belts are regions of lower temperatures, cyclonic vorticity, sinking motions and relatively cloud-free. The belt and zone temperature differences imply that baroclinic energy sources are present. The condition for barotropic (shear) instability appears to be satisfied at the edges of at least some of the belts, and this mechanism is likely to account for at least some of the larger-scale (~ 5000 km) non-symmetric features present in the atmosphere.

Current suggestions for explaining other non-symmetric features and the banded structure and zonal currents require ad hoc *assumptions about the atmospheric structure. To help evaluate such suggestions, it would be particularly valuable to measure meridional velocities; to measure the lapse rate and static stability of the visible cloud layers and the layers immediately below; and to carry out a high-resolution imaging experiment capable of resolving small-scale convection. Theoretical models of the dynamics and structure of the visible cloud layers have not been very successful so far, but models have not been developed for all possible dynamical regimes – e.g., for forced convection and inertial instability regimes. To put theoretical calculations on a firm foundation it will be necessary to determine the latitudinal variation of the internal heating.*

The meteorology of planetary atmospheres other than the earth's is a subject which barely existed ten years ago. Pioneering studies of the circulations of planetary atmospheres, including Jupiter's, were undertaken by the Lowell Observatory in 1948–1952 (Slipher *et al.* 1952) and by Hess and Panofsky (1951) but these studies had few successors. Extra-terrestrial meteorology did not attract widespread interest until the development of spacecraft technology in the mid 1960's provided the necessary stimulus. The subsequent steady increase in spacecraft observations has been accompanied by a steady increase in the number of papers published on extra-terrestrial meteorology. The review article by Goody (1969) and the Confer-

ence on the Motions of Planetary Atmospheres sponsored by the Kitt Peak National Observatory (Gierasch 1970) marked the general acceptance of the subject as one of crucial importance not only to meteorologists, but to all atmospheric scientists. Studies of the meteorology of Mars are already having an impact on our understanding of the earth's atmosphere and climate (Stone 1972*b*, 1973*b*; Sagan *et al.* 1973; Hartmann 1974). Studies of Jovian meteorology can be expected to have a similar impact. The substantial differences between Jupiter's atmosphere and the atmospheres in the inner solar system, e.g., the presence of an internal heat source and the great size of the planet, will provide a stringent test for our understanding of atmospheric motions and how they depend on external parameters.

The study of Jovian meteorology is not yet as advanced as the study of the meteorology of the inner planets. Pioneers 10 and 11 have just begun the collection of the necessary data. As with the inner planets, atmospheric orbiters and probes will be necessary to determine crucial meteorological parameters such as the lapse rate and the latitudinal distribution of the internal heating. Consequently this review will necessarily focus on ideas more than on facts, but these ideas do provide a useful framework for future observations and theoretical studies. Similarly, we will concentrate most of our attention in this chapter on the layers of the atmosphere where we have the most information—namely, the visible cloud layers, where most solar heating occurs, roughly those layers between 300 millibar and 3 bar pressure.

In Sec. I we will review the observations relevant to Jovian meteorology; in Sec. II, the theory of dynamical regimes on rotating planets; in Sec. III, integrated theories of Jupiter's atmospheric structure and dynamics; and in Sec. IV, the dynamics of particular features, such as the zonal currents, the banded structure, and the Great Red Spot. In addition to the review by Goody (1969), earlier reviews of Jovian meteorology have been presented by Hide (1969), Stone (1973*a*), and Maxworthy (1973).

It is convenient to define here the symbols we will be using. They are:

c_p specific heat at constant pressure.
D characteristic vertical scale of the motions.
F flux through the atmosphere.
$\bar{F}_s$ mean flux carried by small scale convection.
f Coriolis parameter $= 2\Omega\sin\phi$.
g acceleration of gravity.
H scale height $= RT/g$.
K_h horizontal eddy diffusion coefficient.
K_v vertical eddy diffusion coefficient.
L characteristic horizontal scale of the motions.
P pressure.
P_0 reference pressure.
R gas constant.

R_0 radius of the planet.
S static stability $= \partial\theta/\partial z$.
T temperature.
u zonal velocity.
v meridional velocity.
w vertical velocity.
x west to east (zonal) coordinate.
y south to north (meridional) coordinate.
z vertical coordinate.
α thermal expansion coefficient $= 1/T$.
β beta parameter $= \mathrm{d}f/\mathrm{d}y$.
Γ adiabatic lapse rate $= g/c_p$.
$\Delta\theta$ potential temperature difference over a depth D $[\theta(z + D) - \theta(z)]$.
ΔT temperature difference between zones and belts.
θ potential temperature $= T(P_0/P)^{R/c_p} \cong T + \Gamma Z$.
ρ density.
τ radiative relaxation time.
ϕ latitude.
Ω angular rate of rotation.

I. OBSERVATIONS

The wealth of detail in the visual appearance of Jupiter exceeds that for any other planet, and has been the subject of investigation for centuries. The observations have been summarized by Peek (1958). The most prominent visual features are the banded structure and the Great Red Spot. These are illustrated schematically in Fig. 1. The bands are symmetric about the axis of rotation, with the lighter bands generally being referred to as "zones," and the darker bands as "belts." The belts are indicated by cross-hatching in Fig. 1, and are labeled according to Peek's nomenclature; e.g., *SSTB* refers to the South-South Temperate Belt. The positions indicated for the edges of the belts in Fig. 1 are the mean positions given by Peek for many apparitions. The equatorial zone is about 20,000 km wide, and the width of the other bands generally decreases with increasing latitude. The groundbased observations suggest that the banded structure disappears in the North and South Polar Regions (labeled *NPR* and *SPR* in Fig. 1), and this has been essentially confirmed by Pioneer 11. Its imaging experiment showed that there was, at most, only vestigial remnants of a banded structure in high latitudes, far less prominent than in low latitudes (Swindell *et al.* 1975).[1]

The Great Red Spot, located in the South Tropical Zone, is the most prominent and most long-lived of the non-symmetric features. Although its

[1]See p. 554.

appearance and visibility vary, typically it is oval, about 12,000 km wide in latitude, and 25,000 km long in longitude. As far as is known, it has been present ever since telescopic observations started in the 17th century. Many smaller non-symmetric features also occur, ranging in size from that of the Great Red Spot, all the way down to the limit of resolution, currently the few hundreds-of-kilometers achieved by Pioneer 11. The Pioneer 10 and 11 imaging experiments (Gehrels *et al.* 1974, Swindell *et al.* 1975)[2] have been especially valuable for obtaining information about these smaller scale non-symmetric features. Particularly noteworthy is the presence of lines of vortices at the boundaries between zones and belts. These have typical diameters of 5000 to 10,000 km, and often give the edges of the bands a wavy appearance.

The presence of all these visual features makes it possible to deduce information about motions in the atmosphere, simply by measuring the features' displacements over a period of time. Peek (1958) has summarized the apparent motions deduced in this fashion. The displacements are almost invariably zonal, i.e., parallel to the equator. The rotation periods deduced for various latitudes are indicated by the *X*'s in Fig. 1, with the scale given on the vertical axis. These periods are again mean values over many apparitions. In some latitudes the measured rotation periods vary considerably, and for these latitudes the *X*'s in Fig. 1 have a vertical bar superimposed, whose length indicates the range of the periods measured. Chapman (1969) has given a particularly useful summary of the apparent rotation periods, showing the latitudinal and time variations in much greater detail than Fig. 1.

The most notable feature in the measured rotation periods is the more rapid rotation of the equatorial regions. The five-minute shorter rotation periods in these regions imply westerly winds—i.e., winds in the direction of rotation—about 100 m sec^{-1} greater than winds in high latitudes. This difference led originally to the introduction of two different systems for measuring longitudinal positions (Peek 1958). In System I positions are based on a rotation period of 35,430.0 sec, corresponding to equatorial regions, and in System II they are based on a rotation period of 35,740.6 sec, corresponding to mid and high latitudes. Subsequently, observations of radio emissions from Jupiter's magnetosphere found that the mean rotation period of the emitting regions was 35,729.8 sec (Newburn and Gulkis 1973).[3] This led to the introduction of a third system for measuring longitudinal positions, System III, which is based on the period of the radio emissions. The rotation period of System III is often interpreted as the "true" rotation period of the planet (Newburn and Gulkis 1973).[3] If we adopt this convention, then the rotation period of System I corresponds to an apparent westerly wind at the equator of 106 m sec^{-1} and the rotation period of System II corresponds to an ap-

[2]See p. 536.
[3]See p. 709.

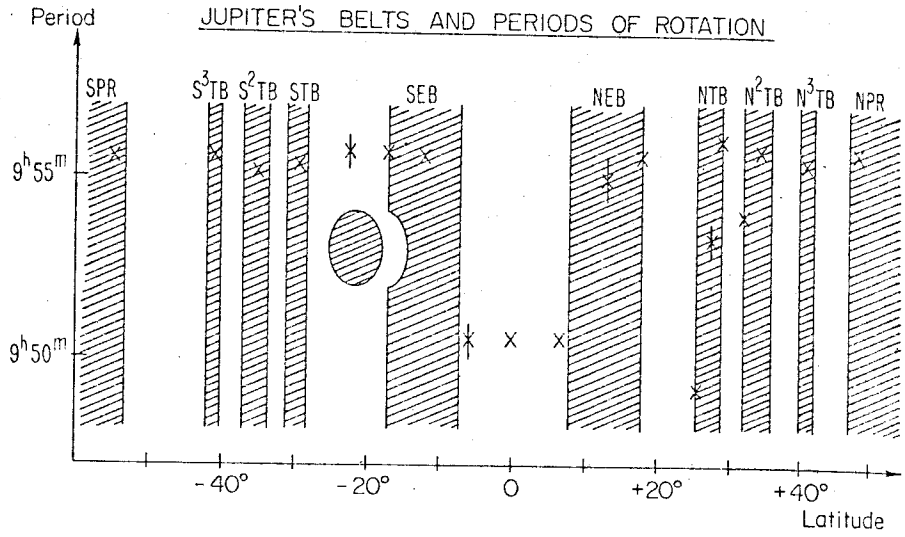

Fig. 1. Jupiter's belts and periods of rotation.

parent easterly wind at higher latitudes, with a speed at 30° latitude, for example, of 3.3 m sec^{-1}. However, there are substantial variations in the apparent velocities at higher latitudes; most notably, the current at the south edge of the North Temperate Belt has an apparent westerly velocity of 123 m sec^{-1}.

Observations of meridional displacements have been very rare (Peek 1958) and it is not yet possible to say anything about mean north-south motions.[4] One particularly noteworthy set of observations which included meridional displacements has been reported by Reese and Smith (1968).[5] They measured the motions of several spots in the vicinity of the Great Red Spot, and found that they tended to circulate around the Spot in a counter-clockwise direction, corresponding to anti-cyclonic vorticity in the southern hemisphere. The measured periods of the circulating spots imply circulatory velocities around the Great Red Spot in the range of 20 to 60 m sec^{-1}.

Measurements of the thermal balance of the planet are particularly important for the meteorology, since the balance tells us something directly about the drives for atmospheric motions. Groundbased observations show that the planet radiates more heat than it absorbs from the sun (Aumann *et al.* 1969) and Pioneers 10 and 11 have confirmed the presence of an internal heat source (Chase *et al.* 1974; Ingersoll *et al.*).[6] The Pioneer 11 measurements should be the most accurate, since they had the best phase coverage. The results indicate that the total heating from the interior is approximately

[4]See, however, p. 554.
[5]See p. 572.
[6]See p. 202.

equal to the total amount of absorbed solar radiation, calculated for a Bond albedo of 0.45. Therefore, the solar heating and internal heating, when averaged over the whole surface of the planet, each supply the atmosphere with about 7×10^3 erg cm^{-2} sec^{-1}. The Pioneer 11 experiment also found that the large scale thermal emissions in high and low latitudes do not differ by more than a few percent (Ingersoll 1976).[7] Since the solar heating is a maximum at the equator, and virtually zero at the poles, this result implies that there is a dynamical transport of heat from equator to pole at some level in the planet.

Knowledge of the atmosphere's temperature structure is also very valuable for analyzing the motions. If the temperature structure were known, one could attempt to solve the equations of motion alone, without having to solve a simultaneous equation for the temperature. Many temperature measurements have been made, but the temperature structure inferred from them is highly model-dependent (Newburn and Gulkis 1973).[8] Brightness temperatures of the belts are generally higher than those of the zones and the Great Red Spot, but there is very little systematic variation of brightness temperatures with latitude or longitude (Westphal 1971; Chase *et al.* 1974; Ingersoll *et al.*).[9] This latter result implies that seasonal and diurnal variations are very small. This is to be expected since the radiative relaxation time of the visible cloud layers of the atmosphere is on the order of 10 Earth years (Gierasch and Goody 1969). The brightness temperatures increase with wavelength, and this implies that the temperature in the atmosphere increases with depth (Newburn and Gulkis 1973). The wavelength dependence of the brightness temperatures is perhaps most useful as a check on the viability of any given model for the atmospheric structure. The models that give the best agreement with the data have near-adiabatic lapse rates in the visible cloud layers, with the clouds being much thicker in the zones than in the belts (Newburn and Gulkis 1973).

II. DYNAMICAL REGIMES ON ROTATING PLANETS

The traditional approach to determining the structure of a planetary atmosphere neglects any differential heating and assumes radiative-convective equilibrium. In this situation, the atmosphere can have two distinct regimes. If the radiative equilibrium temperature profile is statically unstable, small scale convection will arise and prevent the lapse rate from being appreciably superadiabatic. If, on the other hand, the radiative equilibrium temperature profile is statically stable, the atmosphere will be quiescent. This approach is not self-contained, because it is not possible to use the solutions to check the consistency of neglecting the differential heating. Differential heating gives rise to horizontal temperature gradients and large-scale motions, and

[7]See p. 213.
[8]See p. 666.
[9]See p. 213.

these motions tend to stabilize the lapse rate (Stone 1972*a*). The effect of this stabilization is illustrated by the atmospheric structure of the earth and Mars. In mid and high latitudes the lapse rates are substantially subadiabatic, in spite of the fact that the radiative equilibrium profiles are superadiabatic (Stone 1972*b*, Kliore *et al.* 1973). In general, the vertical structure and dynamics of an atmosphere cannot be deduced independently of each other. Of course the large-scale motions also transport heat horizontally and are potentially of crucial importance in determining the horizontal structure of the atmosphere (Gierasch *et al.* 1970).

The importance of Coriolis forces in shaping the motions can be measured by the Rossby number *(Ro)*,

$$Ro = \frac{u}{fL}. \tag{1}$$

In particular, Coriolis forces are dominant if, $Ro \ll 1$. Hide (1963) first pointed out that Ro is generally very small for the large scale motions on Jupiter. For example, at 20° latitude, if we choose $u = 10$ m sec^{-1} as typical. $Ro \ll 1$ provided $L \gg 100$ km. Consequently, we can expect that the large-scale flows will be geostrophic—i.e., horizontal pressure gradients will be balanced by Coriolis forces. The one likely exception to this conclusion is the equatorial current. Taking as typical 4° of latitude, $u = 100$ m sec^{-1}, and $L = 8000$ km, we find $Ro = \frac{1}{2}$ for the equatorial current.

In hydrostatic equilibrium, horizontal pressure gradients imply the presence of horizontal temperature gradients. Consequently, Stone (1967) suggested that the zonal motions on Jupiter arise from meridional temperature gradients and that they are related by the thermal wind relation,

$$f\frac{\delta u}{\delta z} = -\alpha g \frac{\delta T}{\delta y}. \tag{2}$$

Since the derivation of this equation only depends on the assumptions of hydrostatic equilibrium and geostrophy, this relation is a very plausible one for Jupiter. Thermal winds are at right angles to the temperature gradient and, therefore, do not transport heat. However, in geophysical situations these winds are usually unstable, and the resulting instabilities do transport heat and affect the temperature structure. There are a variety of possible instabilities besides small-scale convection that can arise depending on the static stability. Thus, there is a much richer variety of possible atmospheric regimes than is encompassed in the theory of radiative-convective equilibrium.

Figure 2 summarizes these various regimes for a rapidly rotating planet as a function of the Richardson number *(Ri)*, which is a dimensionless measure of the static stability of the atmosphere. Ri is defined as

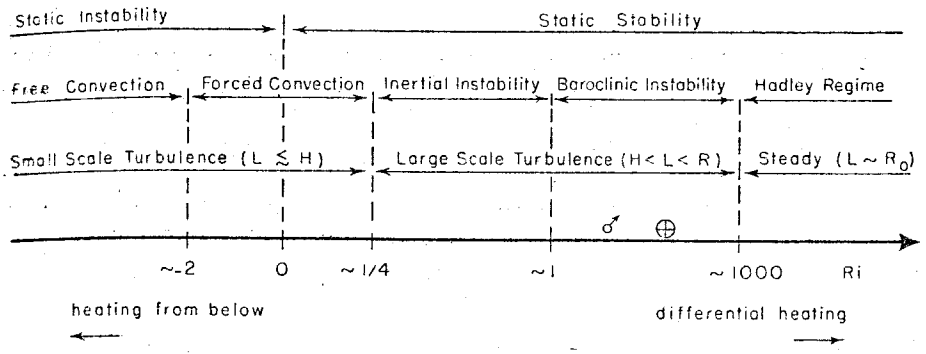

Fig. 2. Dominant heat transporting modes on rapidly rotating planets and their properties.

$$Ri = \frac{\alpha g S}{\left(\frac{\delta u}{\delta z}\right)^2} \sim \frac{\alpha g D^2 S}{u^2}. \tag{3}$$

Figure 2 lists the heat-transporting modes which dominate at different values of Ri, and their properties. If the static instability is sufficiently great, i.e., if Ri is sufficiently negative, then small-scale turbulent convection of the kind invoked in the theory of radiative-convective equilibrium is dominant. In this regime the convection is sufficiently vigorous that its properties are not affected by the horizontal motions arising from differential heating, and by analogy with the theory of turbulence in the terrestrial boundary layer (Priestly 1959), we will refer to this regime as a free convection regime. The characteristic horizontal scales of free convection are generally comparable to the characteristic vertical scales of the atmosphere, although they can be even smaller as, for example, when rotation is very rapid (Chandrasekhar 1961; Roberts 1968).

If the atmosphere is only slightly statically unstable, then the motions driven by differential heating influence the small-scale turbulent convection significantly, although the turbulence is still primarily thermally driven. If the atmosphere is slightly statically stable, then the turbulence is primarily mechanically driven, but still essentially small scale. These two situations, where the static stability is small in magnitude, we will refer to collectively as forced convection, again by analogy with the theory of turbulence in the terrestrial boundary layer (Priestly 1959). The transition point from free to forced convection is not well determined. In the terrestrial boundary layer the most unstable conditions which have been well observed correspond to $Ri \sim -2$, and for this value the convection is still forced rather than free (Businger *et al.* 1971). The value of Ri for this transition in an atmosphere like Jupiter's is of course completely unknown, and we have entered the value -2 in Fig. 2 somewhat arbitrarily. The value of Ri at which flow with

vertical shear ceases to be unstable to small-scale instabilities is predicted by theory to be 0.25 (Drazin and Howard 1966). Observations in the terrestrial boundary layer yield a value for this transition of 0.21 (Businger *et al.* 1971) in good agreement with the theoretical value.

For more stable conditions, $0.25 < Ri < 0.95$, inertial instability is dominant (Stone 1966). This instability draws its energy primarily from the kinetic energy of the thermal wind by means of vertical eddy stresses which tend to destroy the vertical shear of the flow. The unstable perturbations transport heat down the horizontal temperature gradient and upward, and therefore tend to stabilize the atmosphere by increasing the static stability and Ri (Stone 1972*a*). The motions generated are axially symmetric, i.e., independent of longitude.

Under even more stable conditions, $Ri > 0.95$, the dominant instability mechanism is baroclinic instability (Stone 1966). This is the mechanism which produces the extra-tropical cyclones and anti-cyclones observed in the terrestrial and Martian atmospheres. This instability depends on the existence of the horizontal temperature gradients which accompany the thermal winds. These horizontal gradients imply that potential energy is available for perturbations to feed on, even though the atmosphere is statically stable. In particular, a gas parcel which is displaced horizontally into regions of cooler temperatures at the same time that it is displaced upwards, will be buoyant relative to its surroundings and will have its displacement enhanced. Consequently, these instabilities necessarily transport heat down the horizontal temperature gradient and upward, and they also tend to stabilize the atmosphere by increasing S and Ri (Stone 1972*a*). The values of Ri characteristic of the baroclinic instability regimes on Earth and Mars have been calculated by Stone (1972*b*), and are indicated in Fig. 2 by the astronomical symbols for the earth and Mars. In the inertial and baroclinic instability regimes, the characteristic horizontal scales of the motions exceed the characteristic vertical scale of the atmosphere, and systematically increase as Ri increases (Stone 1966).

Finally, for sufficiently large values of Ri, thermal winds are stable, and heat-transporting motions will arise only to the extent that the thermal wind relation is not exact. In particular, dissipative effects will lead to some cross-isobaric flow driven by the differential heating, with poleward flow in the upper layers and equatorward flow in the lower layers, accompanied by rising motions in low latitudes and sinking motions in mid and high latitudes. This kind of flow is referred to as a Hadley regime, and its characteristic horizontal scale is the planetary scale. This stable regime could occur if the characteristic scale of baroclinic instabilities exceeds the planetary scale; if dissipative effects are strong enough; or if the vertical shear of the thermal wind is sufficiently small. Gierasch *et al.* (1970) have estimated that the first two conditions are highly unlikely for Jupiter. The latter condition is given

in quantitative form by Phillips (1951) and can be written in terms of the Richardson number as

$$\frac{\beta u}{f^2} Ri > 2 . \tag{4}$$

For 30° latitude, if we choose $u \sim 10$ m sec^{-1}, this condition becomes $Ri > 1000$, and this is the value of Ri we have entered in Fig. 2 for the transition from a baroclinic instability regime to a Hadley regime. The highly turbulent appearance of Jupiter's atmosphere strongly suggests that its regime is not a Hadley regime.

It should be noted that Fig. 2 does not make any allowances for clouds and condensation. Any of the motions included in Fig. 2 can be expected to lead to clouds and condensation under appropriate conditions. Correspondingly a greater variety of regimes than those indicated in Fig. 2 can be imagined. For example, the earth's tropics are basically a moist convection regime. Barcilon and Gierasch (1970) investigated the thermodynamic consequences of condensates in the Jovian atmosphere. Using Lewis' (1969) solar composition model, they concluded that water was the most important condensate. Current models indicate that the water vapor condensation level is near the 280°K level, about 60 km below the visible cloud layers (Weidenschilling and Lewis 1973). Barcilon and Gierasch showed that the scale height of the saturation vapor pressure near the condensation level is only about 8 km. Consequently the condensation in these layers is unlikely to play a direct role in the dynamics of the visible cloud layers. In the terrestrial atmosphere there are basically two kinds of cumulus clouds (Ogura and Cho 1973). The common variety is low level cumulus, which typically has a vertical extent comparable to the scale height of the saturation vapor pressure. The less frequent variety is deep cumulonimbus towers, which typically have a vertical extent about four times the scale height of the saturation vapor pressure. Even this latter kind of cloud on Jupiter would only reach up to about the 220°K level, still well below the visible cloud layers. Stratus clouds are thermodynamically less active than cumulus clouds.

In the visible cloud layers the only appreciable condensate is ammonia (Lewis 1969). For a solar composition atmosphere, ammonia condensation has a much smaller effect than water vapor condensation in the earth's atmosphere. For example, ammonia condensation only changes the adiabatic lapse rate by 5% and the ammonia saturation vapor pressure curve at the condensation level has a scale height only about one tenth of the atmospheric scale height (Weidenschilling and Lewis 1973), whereas the same factors for water vapor in the earth's atmosphere are 50% and one third.

Consequently the array of regimes presented in Fig. 2 provides a convenient framework for discussing Jupiter's dynamical regime. This array of regimes is consistent with laboratory experiments with rotating fluids (Stone

et al. 1969; Hadlock *et al.* 1972). Non-heat-transporting modes such as barotropic instability have been excluded from Fig. 2, because they do not depend explicitly on Ri and can occur in any of the regimes listed.

Heating from below tends to decrease the static stability of an atmosphere and so an internal heat source tends to drive the dynamical regime towards the left in Fig. 2. On the other hand, differential heating drives motions which tend to stabilize the atmosphere, and so differential solar heating tends to drive the dynamical regime towards the right in Fig. 2. Differential solar heating is stronger in high latitudes than in low latitudes so more stable regimes may occur in high latitudes. The regime will also depend on any differential heating present in the interior heat source. All the models, that we shall discuss in the next section, assume that the atmosphere is heated uniformly from below. The recent Pioneer 11 observations of thermal emissions (Ingersoll 1976) cast doubt on this assumption.

Figure 2 suggests two kinds of observations that would be particularly valuable in determining Jupiter's dynamical regime. One would be measurements of the static stability of the atmosphere so that Ri can be estimated. The other would be a high-resolution imaging experiment, capable of resolving scales $L \sim H$, so as to determine whether small-scale convection is present.

It is convenient to summarize here the characteristics of some of the dynamical modes that are included in Fig. 2 and that we shall be referring to frequently in the next two sections. This summary is presented in Table I. The tabulated criteria for instability are actually the necessary conditions for instability, but for geophysical fluids they are usually also sufficient. Note that these conditions do not necessarily correspond to the conditions under which each mode will be dominant, i.e., different modes can occur simultaneously. The characteristic time scales given in Table I are just the inverse growth rates for the most unstable eigenfunction for each kind of instability.

III. INTEGRATED THEORIES OF JUPITER'S ATMOSPHERIC STRUCTURE AND DYNAMICS

Since dynamical transports influence Ri, the atmospheric regime resulting from specified differential and internal heating is determined by highly nonlinear processes. Consequently, it is usually not possible to obtain a simultaneous solution to the equations of motion and the equations for the temperature structure without restricting the values of Ri *a priori*. In this section we will discuss those models which calculate both temperature structure and properties of the motions after making such a restriction. We shall discuss in separate subsections calculations of radiative-convective equilibrium, calculations of large scale motions in the free convection regime, and calculations for a baroclinic instability regime.

TABLE I

Properties of Dynamical Modes

Dynamical Mode (source)	Criteria for Instability	Structure	Characteristic Horizontal Scale	Characteristic Time Scale
barotropic instability (Kuo 1949)	$\frac{d^2u}{dy^2} > \beta$	three dimensional	$\pi\left(\frac{u}{\beta}\right)^{\frac{1}{2}}$	$\frac{10}{(u\beta)^{\frac{1}{2}}}$
baroclinic instability (Stone 1966, 1970)	$Ri > 0.84$	three dimensional	$2\frac{u}{f}(1+Ri)^{\frac{1}{2}}$	$\frac{3}{f}(1+Ri)^{\frac{1}{2}}$
inertial instability (Stone 1971)	$Ri < 1$	axially symmetric	$2\left(\frac{u}{\beta}\right)^{\frac{1}{2}}\left(\frac{Ri^2}{1-Ri}\right)^{\frac{1}{4}}$	$\frac{1}{f}\left(\frac{Ri}{1-Ri}\right)^{\frac{1}{2}}$
radiative instability (Gierasch 1973)	(see text)	axially symmetric	$2\frac{(\alpha g H^2 S)^{\frac{1}{4}}}{\beta^{\frac{1}{2}}}$	$\frac{\tau}{2}\alpha HS$
free convection (Priestley 1959; Spiegel 1971)	$S < 0$	three dimensional	$\sim H$	$\sim (\alpha g\lvert S\rvert)^{-\frac{1}{2}}$

(a) *Radiative-convective Equilibrium*

Calculations of radiative-convective equilibrium for Jupiter have been published by Trafton (1967), Hogan *et al.* (1969), Divine (1971), and Trafton and Stone (1974). In these calculations the radiative equilibrium structure is modified by supressing superadiabatic lapse rates. Since the effect of large scale motions is not included, these calculations implicitly assume that the dynamical regime is a free convection regime. The convection could be either dry or moist; in the calculations the adiabatic lapse rate is taken to be the moist adiabatic lapse rate in regions where a significant condensate is present.

Typically in these calculations the lapse rate becomes adiabatic at $T \sim 140°\text{K}$, $P \sim 500$ mb. Consequently, in these models the visible cloud layers of the atmosphere are mainly convecting, with lapse rates $\sim 2°$ per km. The horizontal temperature gradients in radiative-convective equilibrium are the same as in radiative equilibrium and these latter gradients have been calculated by Stone (1972*b*). If the internal heating is comparable to the solar heating, in the visible layers at 45° latitude the gradient is 3° per 10^4 km. This value represents an upper bound to the mean gradients that would result if dynamical transports were taken into account and is dependent on the assumption that the heating from below is uniform.

If the convection is dry, its properties can be estimated from free convection theory and mixing length theory (Priestly 1959; Spiegel 1971). The characteristic space and time scales are given in Table I, and from these the characteristic velocity can be estimated to be

$$w \sim (\alpha g |S|)^{\frac{1}{2}} H \,. \tag{5}$$

According to mixing length theory, the flux is given by

$$F \sim -\rho c_p w H S \,. \tag{6}$$

Solving for S and w in terms of F, we find

$$w \sim \left[\frac{R}{c_p}\frac{F}{\rho}\right]^{\frac{1}{3}} \tag{7}$$

$$S \sim -\frac{w^2}{HR} \,. \tag{8}$$

Barcilon and Gierasch (1970) used these equations to estimate S in the visible cloud layers. They found $|S| \sim 6 \times 10^{-10}$ °K per cm. They combined this value with the u velocity scale observed in the visible cloud layers and estimated Ri. With values of $u = 30$ m sec^{-1}, $D = 80$ km, they calculated $Ri = -4 \times 10^{-3}$ and concluded that the visible cloud layers could not be in free convection. This calculated value of Ri is so small compared to the minimum critical value of -2, that it appears to be a very strong conclusion.

It is still possible that in lower layers, below the regions of differential solar heating, $\partial u/\partial z$ becomes small enough that free convection can occur.

As Barcilon and Gierasch point out, in the layers immediately below the visible cloud layers, near the 300°K level, condensation of water vapor is important. One would expect convection in these layers to be essentially moist convection, with a significant fraction of the heat flux carried as latent heat rather than as sensible heat. The moist adiabatic lapse rate in these layers is near 1°5K per km, and the dry adiabatic lapse rate is near 1°8K per km. Consequently, these layers could exhibit a static stability ~ 0°3K per km. Clearly the determination of the lapse rates in the visible cloud layers, and in the layers where water condensation can be expected is a prime objective of a probe mission. A static stability of 0°3K per km should be measurable by such an experiment.

At lower layers free of condensates, dry free convection might still occur. Near the 400°K level, Eqs. (7) and (8) yield estimates of $w \sim 2$ m sec^{-1} and $S \sim -2 \times 10^{-10}$°K per cm. The corresponding characteristic time scale would be 7 hours. Since the characteristic horizontal and vertical scales are the same in free convection, the eddy diffusion coefficients can be estimated from the relation

$$K_h \sim K_v \sim wH\,. \tag{9}$$

Their value at these levels would be ~ 10^9 cm^2 sec^{-1}. Since the characteristic time scale at this level is comparable to the period of rotation, free convection would be influenced by Coriolis forces. However, at these levels this influence would not be strong enough to change the order of magnitude of the above estimates.

At deeper levels, as ρ increases, the characteristic time scale increases, and the influence of Coriolis forces would become more and more dominant. Robert's (1968) and Busse's (1970*a*) analyses of convection in a rapidly rotating deep atmosphere indicate that the amplitude of the convection on a spherical surface is a strong function of latitude. This result suggests the possibility that the flux of heat from the interior into the visible cloud layers is not uniform in latitude, and emphasizes the need for determining its distribution. Such differential heating would imply horizontal temperature gradients, horizontal motions, and horizontal heat transports in the deep atmosphere. These properties could explain the Pioneer 11 observation that thermal emissions in high latitudes are just as strong as those in low latitudes, in spite of differential solar heating. Clearly, an analysis of the finite amplitude, rotating convection problem for a deep atmosphere would make an important contribution to our understanding of Jupiter's atmosphere.

(b) Large-scale Motions in Free Convection

Williams and Robinson (1973) studied the hypothesis that the large-scale motions and structure of Jupiter's atmosphere are convectively driven—i.e., that small-scale convection driven by the internal heat source has a large-scale organization that can explain the observations. To check this

hypothesis they integrated the Boussinesq equations of motion and temperature in a statically unstable, rotating spherical shell. The dominant small-scale convection was parameterized with simple eddy diffusion laws, and only the large-scale motions were explicitly calculated.

Williams and Robinson had four parameters in their model which they regarded as free parameters: the depth of the spherical shell, D; the amount by which the potential temperature of the lower surface exceeded that of the upper surface, $\Delta\theta$; and the vertical and horizontal eddy diffusion coefficients, K_v and K_h, respectively. Consequently, they performed a parameter study in which they sought values for these parameters that would give solutions resembling Jupiter's circulations. In this parameter study they neglected differential heating, and therefore were studying essentially a free convection regime. They also assumed that the motions were axially symmetric. They found that there were values of these four parameters which enabled them to match the observed strength and width of the equatorial current, and the observed scale and extent of the banded structure. In particular, in the model which fit the observations best, their model *PBJ*, the parameter values were $D = 50$ km, $\Delta\theta = 133°$, $K_v = 10^7$ cm^2 sec^{-1}, and $K_h = 10^{13}$ cm^2 sec^{-1}. In addition, the solutions showed features which agreed with the observations even though the parameter values were not specifically picked to fit them. For example, the scale of the banded structure decreased poleward, and the vorticity had the correct correlation with the belts and zones. The considerable agreement between many of the details of their solution and the observations has been cited by Gehrels (1974) in support of the hypothesis that the motions are essentially convectively driven.

However, there is one observable quantity which Williams and Robinson did not use to constrain their parameter study, namely, the energy flux through the atmosphere. The flux in their model is given by

$$F = \rho c_p (w\theta - K_v S) . \tag{10}$$

As one would expect for free convection, the main term contributing to this flux in their solutions is the second term, which gives the flux carried by the small-scale parameterized convection. If we average the second term vertically, then we obtain

$$\bar{F}_s = \rho c_p \frac{K_v \Delta\theta}{D} . \tag{11}$$

If we use the parameter values from their model *PBJ*, and choose $\rho = 1.6 \times 10^{-4}$ g cm^{-3} and $c_p = 1.4 \times 10^8$ erg per °K per gram as typical of the visible cloud layers, we calculate $\bar{F}_s = 6 \times 10^6$ erg cm^{-2} sec^{-1}. This is three orders of magnitude larger than the observed value $\sim 10^4$ erg cm^{-2} sec^{-1}. If one attempts to change the values of K_v, $\Delta\theta$, and D in order to reduce this flux, then as Williams and Robinson showed, in order to maintain the dynamical similarity of their solutions one must keep $D\Delta\theta$ and D/K_v constant, and $D <$

500 km. Consequently, one can reduce the flux in their solutions by only one order of magnitude, without losing the resemblance to Jupiter's circulations.

In the face of this discrepancy, it is difficult to argue that Jupiter's dynamical regime is basically a convective regime driven by the internal heat source. Williams and Robinson's calculations indicate that the known strength of this heat source is too weak to account for the observed circulations. This suggests that differential heating must play a role in driving the motions, and that Jupiter's dynamical regime will be one of the more stable ones listed in Fig. 2.

This conclusion is in accord with Barcilon and Gierasch's (1970) conclusion cited above, that free convection is not consistent with the observed horizontal velocity magnitudes. In fact, the parameter values calculated in the preceding section from free convection theory are quite different from the values that Williams and Robinson found necessary in order to match the observed circulations. In particular, the values estimated from free convection theory were $K_h \sim K_v \sim 10^9$ cm^2 sec^{-1} and $\Delta\theta \sim 2 \times 10^{-3}$°K, in contrast to the necessary values $K_h \sim 10^{13}$ cm^2 sec^{-1}, $K_v \sim 10^7$ cm^2 sec^{-1} and $\Delta\theta \sim 133$°K. According to Williams and Robinson's results, the former values would make the large scales convectively stable—i.e., the Rayleigh number would be subcritical and there would be no large scale motions driven by uniform internal heating.

There are also theoretical difficulties with the convective model. One is the prescribed axial symmetry. Other analyses of convection in a rotating, spherical system show that the dominant convective modes are not axially symmetric (Roberts 1968; Busse 1970*a*,*b*). In fact, Williams and Robinson reported that when they perturbed their axially symmetric solutions which matched the observations best, the symmetric convection cells broke up into non-symmetric cells. Another difficulty, pointed out by Williams and Robinson, is the very large values of K_h needed to match the observations. Since the velocities in the solutions were $u \lesssim 100$ m sec^{-1}, the value $K_h \sim 10^{13}$ cm^2 sec^{-1} corresponds to mixing lengths $L \geq 10{,}000$ km. Since these are comparable to the characteristic scales of the large-scale motions, it is not consistent to parameterize the small-scale motions by eddy diffusion laws.

(c) *Baroclinic Instability Regime*

Stone (1972*b*) has calculated the atmospheric structure that would occur in the visible cloud layers if baroclinic instabilities were the main source of dynamical heat transport. His model gives qualitatively good results when applied to the earth or Mars (Stone 1972*b*), but it neglects deep atmosphere effects and, therefore, has to be interpreted cautiously when applied to Jupiter. McIntyre (1972) has shown that baroclinic instability in general still occurs in a deep atmosphere, but the growth rates are reduced. In particular, some of the available potential energy is diverted into driving motions in the

lower, non-baroclinic layers, with the division of energy between the baroclinic and non-baroclinic layers being inversely proportional to the static stability of the respective layers. If the static stability of the non-baroclinic layers is comparable to, or greater than, that of the baroclinic ones, then Stone's model should give qualitatively reasonable results. However, if the static stability of the non-baroclinic layers is smaller, then the instability of the baroclinic ones will be reduced, and perhaps even eliminated in extreme cases. In this case, the stabilizing effect of the instabilities on the temperature structure of the baroclinic layer could be decreased or even removed, and correspondingly, Stone's model can only be interpreted as giving upper bounds to S and Ri in the baroclinic layer.

Stone (1972*b*) calculated equilibrium states for 45° latitude and found that the value of Ri was so sensitive to external parameters that no conclusions could be drawn about the dynamical regime. For example, decreasing the internal heat source by 50% changed Ri from values < 1 to values ~ 10. However, it was also found that the static stability is extremely small, even if one allows for the uncertainty in the external parameters. For example, in the most stable possible baroclinic instability regime Stone calculated $S \sim 3 \times 10^{-3}$ °K per km. Since this very small value represents an effective upper bound on the static stability of the visible cloud layers, one can conclude that the lapse rate in these layers should be very nearly adiabatic, and calculations of radiative-convective equilibrium should give good results for the vertical structure of these layers. In addition, these very small values suggest that deep atmosphere effects may not seriously affect the predictions of Stone's model after all. Judging from the earth's tropics, regions in which moist convection occurs act dynamically as though they were statically stable. In other words, the areas of active moist convection cover only a few percent of the total area (Ogura and Cho 1973), but this is sufficient to produce a mean lapse rate over the whole area which is nearer the moist adiabatic lapse rate than the dry adiabatic lapse rate. Such a layer of moist convection on Jupiter near the 300°K level would exhibit a static stability ~ 0.3 K and this would be sufficient to make Stone's model valid for the visible cloud layers.

Trafton and Stone (1974) pointed out that the sensitivity of Ri to the external parameters implied a strong change in the equilibrium value of Ri with latitude. They used Stone's model to calculate Ri as a function of latitude and found that $Ri < 1$ in low latitudes and $Ri > 1$ in high latitudes, and that uncertainty in the external parameters primarily introduces uncertainty in the latitude of the critical value, $Ri = 1$. Using the value of Aumann *et al.* (1969) for the strength of the internal heat source, 1.3×10^4 erg cm^{-2} sec^{-1}, they estimated that this latitude was $\sim 70°$. If their calculation is re-done using the Pioneer 11 value for the strength of the internal heat source, 7×10^3 erg cm^{-2} sec^{-1}, (Ingersoll)[10] and assuming that the 170°K level is typical

[10]See p. 202.

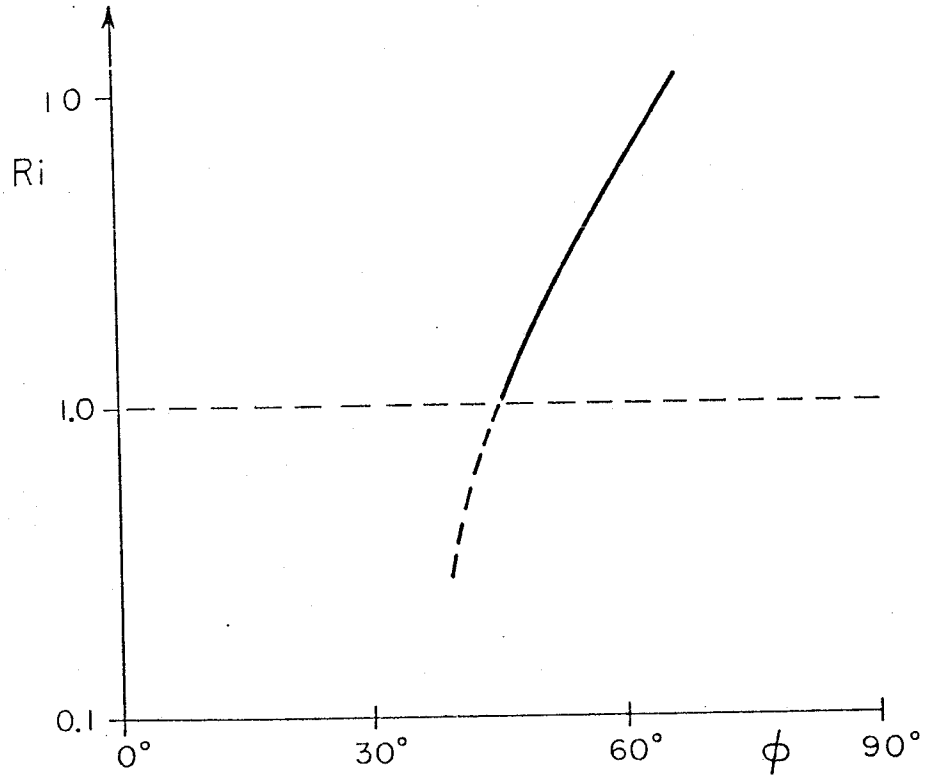

Fig. 3. Variation of equilibrium Richardson number with latitude.

of the visible cloud layers, then the variation of Ri with latitude changes to that given in Fig. 3. Now the critical latitude is $\sim 45°$. The part of the curve in Fig. 3 corresponding to values $Ri < 1$ is dotted to indicate that Stone's model formally breaks down for these values, because baroclinic instabilities cease to be the dominant heat-transporting mechanism (see Fig. 2).

Trafton and Stone's calculation shows that in low latitudes baroclinic instabilities, even if they could occur, could not be sufficiently stabilizing to produce a baroclinic instability regime. This result implies that Jupiter's dynamical regime in low latitudes is one of the less stable ones listed in Fig. 4. This destabilization of Jupiter's atmosphere compared to the earth's and Mars' is a consequence of the much weaker horizontal temperature gradients in Jupiter's atmosphere. These gradients are smaller than on the earth or Mars mainly because the solar differential heating is spread out over a much greater planetary scale, and secondarily, because of the (assumed) lack of differential heating associated with the internal heat source. These gradients are the primary drive for baroclinic instabilities, and thus on Jupiter they would be relatively weaker and less efficient at stabilizing the temperature

structure. The breakdown of the baroclinic instability model in low latitudes combined with the difficulties inherent in assuming a free convection regime suggest that Jupiter's dynamical regime in low latitudes is one of the intermediate regimes listed in Fig. 2. Consequently it would be highly desirable to develop integrated models for the dynamics and temperature structure of forced convection and inertial instability regimes. A start has been made toward such a model for an inertial instability regime by Walton (1975), but his analysis is concerned only with the monotonic symmetric instability mode, which is subdominant when $Ri < 1$.

Trafton and Stone's calculation still leaves open the possibility of a baroclinic instability regime in high latitudes. The prediction inherent in Fig. 3, that the regime should change over to a more stable, non-symmetric regime poleward of 45° latitude, is in good agreement with the observed change-over from a predominantly symmetric to a predominantly non-symmetric regime at 50° latitude (Gehrels, p. 537). Figure 3 implies that a typical value of Ri in high latitudes would be ~ 10. The corresponding value for the characteristic scale given in Table I for baroclinic instabilities at 60° latitude, with $u \sim 10$ m sec^{-1}, would be 800 km. This scale refers specifically to the half-wavelength in the downstream direction of the most rapidly growing baroclinic perturbations. This value appears to be typical of many of the features seen in the high-latitude pictures obtained by Pioneer 11.

However, Stone's (1972*b*) calculations also show that horizontal heat fluxes by baroclinic instabilities in the visible cloud layers have a negligible effect on meridional temperature gradients. This result does not rule out the possibility that there are significant meridional transports in deeper layers, and in fact, the Pioneer 11 observation that the thermal emissions are independent of latitude requires just such a transport. This implies that the visible cloud layers are subjected to greater heating from the interior in high latitudes than in low latitudes. Since all the calculations with Stone's model assumed that the heating from the interior was uniform in latitude, one must consider how an internal heat source that increases with latitude affects the conclusions based on his model. Such an increase with latitude will oppose differential solar heating, and, therefore, will lead to weaker mean meridional temperature gradients than one would expect if the internal heating were uniform. This will weaken the drive for baroclinic instabilities, and in particular, will decrease the stabilizing effect of the instabilities on S and Ri. Therefore, the conclusions that the visible cloud layers will be very nearly adiabatic and that the low latitude regime is less stable than a baroclinic instability regime are merely reinforced if the internal heating does indeed increase with latitude. On the other hand, such an increase with latitude shifts the curve in Fig. 3 toward the right and this decreases the chance that the high latitude regime is a baroclinic instability regime. To assess this possibility more accurately, information about the latitudinal variation of the internal heating in high latitudes is needed.

IV. DYNAMICS OF INDIVIDUAL FEATURES

In this section we review dynamical investigations which attempt to explain particular features of the Jovian circulations without placing them within the context of a complete theory of the general circulation and structure of the atmosphere. We shall consider these investigations under four general headings: zonal motions, the banded structure, the Great Red Spot, and nonsymmetric features. It will be convenient again to refer to Table I for the important characteristics of the dynamical modes to which we will be referring frequently.

(a) Zonal Motions

As we discussed in Sec. II, the zonal winds are likely to be thermal winds, obeying the thermal wind relation. Eq. (2). Stone (1967) pointed out that this relation implies that vertical shear is present in the zonal flow, and this complicates the interpretation of measured zonal wind profiles such as that shown in Fig. 1. The apparent latitudinal variations may be caused by vertical variations as well as by horizontal ones. Another difficulty in interpreting the measured motions has been emphasized by Maxworthy (1973) and Stone (1974). We cannot be sure whether the measured velocities refer to phase velocities or to true mass motions. For example, barotropic Rossby waves with characteristic horizontal scale, L, propagate in the zonal direction with a phase speed given by (Holton 1972)

$$c = u - \frac{\beta L^2}{2\pi^2} . \tag{12}$$

Thus, a wave at 30° latitude with $L = 5000$ km would propagate 5 m sec^{-1} more slowly than the actual mean flow. Stone (1974) has suggested that this lag could account for the mean lag of System II motions behind System III.

These uncertainties in interpreting the measured velocities indicate that one should not put too much credence in the details of measured velocity profiles. Only the major features, such as the equatorial current and the current at the edge of the North Temperate Belt are likely to be reliable. The equatorial current has attracted particular interest because it appears to have greater angular momentum than either the underlying atmosphere or the atmosphere in higher latitudes (Hide 1970). This raises the problem of how the current is maintained against small scale diffusion. In particular, the diffusion of momentum must be balanced either by an equatorward transport or by an upward transport of momentum by atmospheric motions. An equatorward transport would imply a negative correlation between u and v on the north edge of the current and a positive correlation on the south edge. Observations of meridional motions that can yield information about such correlations would be particularly valuable.

Three mechanisms for supplying an equatorward transport have been suggested: inertial instability (Gierasch and Stone 1968); baroclinic instability (Stone 1972*a*); and convection under the influence of rotation (Busse 1976). The viability of the first mechanism for supplying the required transport has been discussed extensively (McIntyre 1970; Hide 1970; Stone 1972*a*; Maxworthy 1972; Gierasch and Stone 1972). Here it is sufficient to note that inertial instability can supply the required transport only under the rather limited circumstance that $0 < Ri < \frac{1}{3}$, and it cannot account for any acceleration relative to the underlying atmosphere. Baroclinic instability can supply the required transport so long as $Ri = 0(1)$ and it can account for an acceleration relative to the underlying atmosphere; it therefore is a more plausible mechanism than inertial instability. However, our ignorance of actual values of Ri in the Jovian atmosphere still makes this mechanism a speculative one.

Perhaps the most plausible for an equatorward transport is the convection mechanism. This has also been invoked to explain the solar differential rotation (Busse 1970*b*), and it has been observed to operate in laboratory experiments (Busse 1976). The dominant convective modes in a rotating, self-gravitating system are non-axisymmetric cells (Roberts 1968; Busse 1970 *a*,*b*). Coriolis forces act to deflect the zonal motions in these cells towards the right in the northern hemisphere, and towards the left in the south, thereby creating an eddy flux of zonal momentum towards the equator. Since the visible cloud layers are predominantly axisymmetric, Busse (1976) suggests that the non-axisymmetric cells operate in the deep atmosphere to produce a deep equatorial current, and that the equatorial acceleration observed in the visible cloud layers is forced by this deep current. Again, the need for an analysis of the finite amplitude, rotating convection problem in a deep atmosphere is apparent.

One mechanism for generating the equatorial current by means of an upward transport of momentum at the equator has also been proposed. Maxworthy (1975) has suggested that equatorially-trapped Kelvin waves and mixed Rossby-gravity waves are generated in the lower atmosphere and propagate upwards carrying zonal momentum. Then they are dissipated in the upper atmosphere, deposit their momentum, and generate a mean current. This mechanism has been invoked previously to explain the equatorial currents in the terrestrial stratosphere (Holton and Lindzen 1972). Invoking this mechanism to explain the Jovian equatorial current does require, however, *ad hoc* assumptions about the generation and dissipation of equatorial waves.

Some other recent studies in fluid dynamics have interesting implications for Jupiter's equatorial current. Whitehead (1975) performed experiments with a barotropic rotating fluid on a β-plane. He found that *any* localized stirring of the fluid produced a westerly jet at the latitude of the stirring. Lorenz (personal communication) has found the same result in a numerical study of a barotropic atmosphere on a rotating, spherical surface. In particu-

lar, even an equatorial jet can be produced if the stirring occurs at the equator. The mechanism at work here is not clear, but the results are in accord with terrestrial experience, where the stirring mechanism for generating the mid-latitude westerly jet can be regarded as baroclinic instability. These results suggest that the fundamental problem in explaining Jupiter's equatorial current may not be explaining the current *per se*, but rather determining what stirring mechanism operates near the equator.

One feature of the equatorial current can be explained without relying on any particular dynamical mechanism for generating it. Hide (1966) pointed out that the width of the equatorial current (and similarly of the equatorial zone) can be deduced simply from scaling analysis. It should have a half-width of order

$$L \sim \left(\frac{u}{\beta}\right)^{\frac{1}{2}} \tag{13}$$

For $u = 100$ m sec^{-1}, this formula yields $L \sim 4000$ km, in reasonable order-of-magnitude agreement with the observed half-width, ~ 8000 km.

(b) Banded Structure

Hess and Panofsky (1951) presented the first dynamical discussion of the bands. They noted that the measurements of apparent zonal motions indicate that $\frac{1}{f}\frac{\partial u}{\partial y}$ is positive in zones and negative in belts; i.e., the zones tend to be regions of anticyclonic vorticity, and the belts, regions of cyclonic vorticity. This correlation is particularly clear between 20°S and 30°N latitudes (see Fig. 1). Since the zonal motions appear to be geostrophic, i.e., they satisfy the relation

$$fu = -\frac{1}{\rho}\frac{\delta P}{\delta y}, \tag{14}$$

this correlation implies that the zones are regions of high pressure, and the belts regions of low pressure. This, in turn, implies that there will be meridional flow from the zones to the belts, and since presumably we are looking at high levels in the atmosphere, continuity requires that the zones be regions of rising motions, and the belts regions of sinking motions. Since rising motions favor cloud formations, one would expect from these dynamical arguments that the zones would be relatively cloudy and the belts relatively clear. This picture of the meridional circulations is illustrated schematically in Fig. 4. Hess and Panofsky's picture is convincing, since it is supported by observations of lower albedos in the belts, as one would expect for relatively cloud-free areas; by observations of higher-brightness temperatures in the belts, as one would expect if the thermal radiations were coming from deeper layers; and by theoretical calculations of infrared spectra (Newburn and Gulkis 1973).

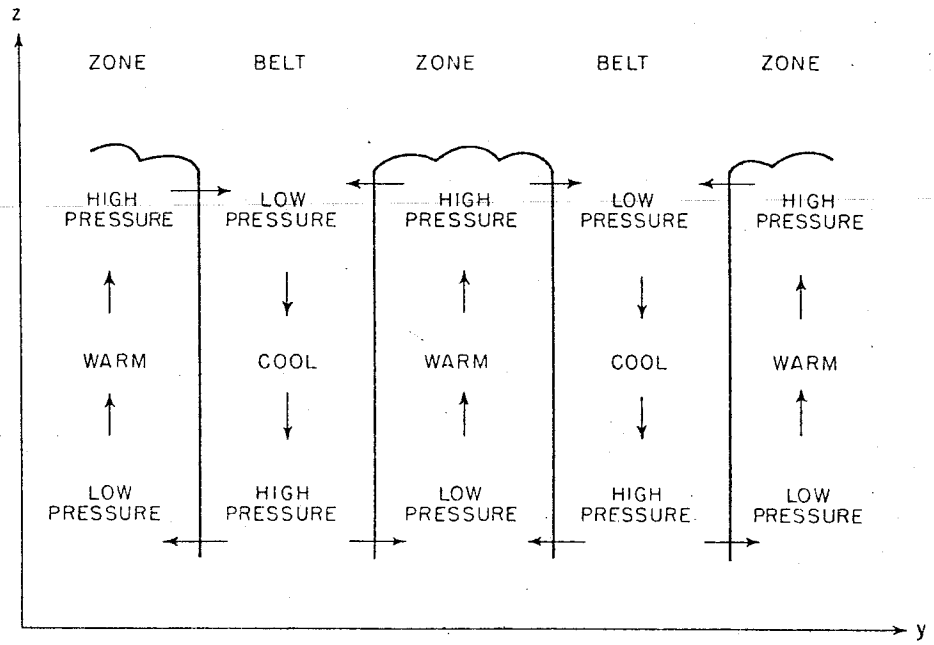

Fig. 4. Schematic diagram of Jupiter's meridional circulations.

Ingersoll and Cuzzi (1969) showed that the correlation between the vorticity and the banded structure also implies a correlation between temperature and the banded structure because of the thermal wind relation. In particular, they deduced that the zones are warmer than the belts. This property is consistent with the picture of rising motions in zones and sinking motions in belts, and has also been included in Fig. 4. Ingersoll and Cuzzi calculated that the temperature difference between the zones and belts is given by

$$\alpha \Delta T D \sim 1.2 \text{ km}. \tag{15}$$

For example, if $\alpha = (180°\text{K})^{-1}$ and $D = 50$ km, then $\Delta T = 4°\text{K}$. They also noted that these local variations appear to dominate any systematic variation of temperature with latitude.

Barcilon and Gierasch (1970) suggested that the higher temperatures in the zones could be caused by condensation there. They found, using Lewis' (1969) solar composition model for the condensates, that this condensation could produce temperature differences on the order of those deduced by Ingersoll and Cuzzi—specifically, $\Delta T \sim 2°$ at the condensation level. They then constructed a model in which the meridional circulations and banded structure were generated by this condensation. Their model was not closed, so they could not solve for the temperature contrast or the distance between

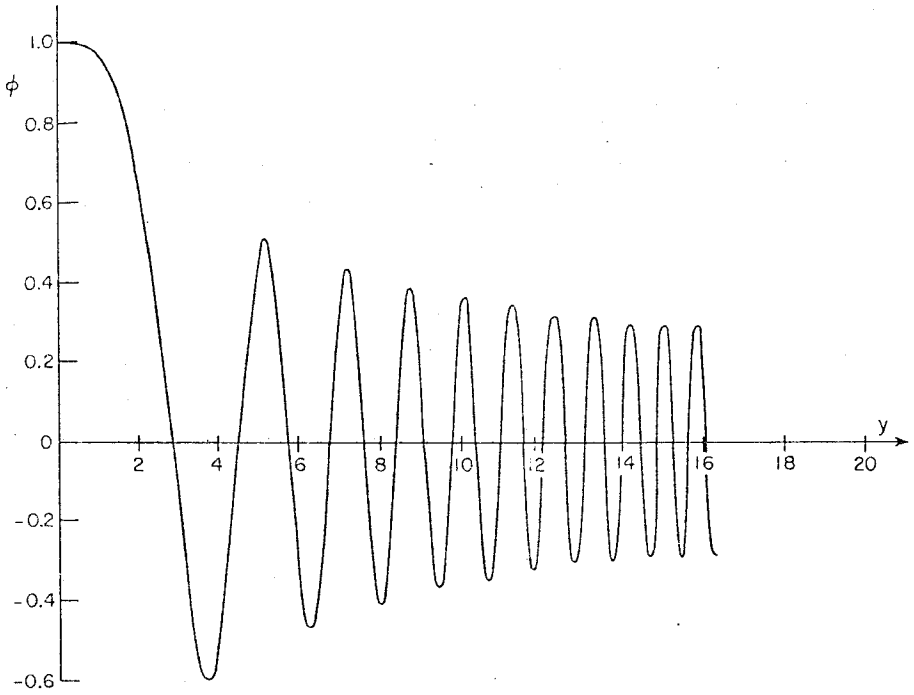

Fig. 5. Amplitude of meridional stream function vs. latitude for inertial instability (after Stone 1971).

zones and belts. In addition, they had to assume the axial symmetry, and the motions they describe are unstable—for example, the condition for inertial instability is satisfied. Also, as discussed in Sec. II, it is not clear how the thermodynamic effect of the water vapor condensation could be felt in the visible cloud layers, some 60 km above the condensation level.

Two instability mechanisms have been suggested for forming the banded structure. Inertial instability, described in Sec. II, generates motions which are axially symmetric, and consequently Stone (1967) suggested that this instability might be the cause of the banded structure. The meridional circulations generated by this instability tend to parallel the isentropes, and have very rapid oscillations perpendicular to the isentropes. On a spherical surface these oscillations have a large scale modulation (Stone 1971). Fig. 5 illustrates the amplitude of the modulation for the inertial instability mode that dominates in low latitudes. The characteristic scale given in Table I for inertial instability is the distance from the equator of the first zero in this modulation function.

These motions generated by inertial instability can be described as a kind of small-scale turbulence, modulated as a function of latitude. Where the

modulation has a large amplitude, turbulence is strong and cloud formation will be favored, and where the modulation has a small amplitude the turbulence and cloud formation will be suppressed. Fig. 5 shows that the resulting cloud structures would closely resemble Jupiter's banded structure—i.e., the bands become systematically smaller and less pronounced as one moves away from the equator. The prime assumption that one has to make in invoking this mechanism is that atmospheric conditions will favor this kind of instability, i.e., $\frac{1}{4} < Ri < 0.95$ (Stone 1966). Given this restriction on Ri, the theory predicts a banded structure that is correct quantitatively as well as qualitatively. For example, choosing $u = 100$ m sec^{-1}, the corresponding range of scales for inertial instability (see Table I) is 9000 to 32,000 km, in good agreement with the observed distance from the equator to the center of the equatorial belts, $\sim$ 15,000 km. Comparing the formula for this scale in Table I with Eq. (5), we see that this scale is essentially the one deduced by Hide (1966) from scaling analysis.

The results quoted above for inertial instability strictly apply to the case of no horizontal shear in the mean flow. Some effects of horizontal shear are known. For example, a more accurate condition than that given in Table I for when inertial instability occurs is (Stone 1971)

$$Ri < \frac{1}{1 - \frac{1}{f}\frac{\partial u}{\partial y}}. \tag{16}$$

Therefore, the instability is favored in regions of anticyclonic vorticity. The observed correlation between the vorticity and the banded structure then suggests that inertial instability might be producing or contributing to the banded structures *locally*, in contrast to the global view suggested above. In particular, given a zonal wind profile like the one observed, regions of anticyclonic vorticity will favor inertial instability, which will tend to generate turbulence and cloudiness consistent with the observed correlation of bright zones with regions of anticyclonic vorticity. In any case, ignorance of actual values of Ri makes this mechanism a speculative one. Again we are reminded of the need to develop models for inertial instability regimes capable of predicting temperature structure as well as motions.

Another instability mechanism for generating the bands has been proposed by Gierasch (1973). This is the radiative instability mechanism first discussed by Gierasch *et al.* (1973). If the clouds contain a condensate which enhances the greenhouse effect, then instability is possible; rising motions lead to condensation, which warms the atmosphere locally by increased thermal blanketing and this warming will enhance the rising motions. Gierasch's (1973) analysis of this instability showed that the dominant modes in low latitudes were axially symmetric, with structures very similar to that illustrated in Fig. 5. In addition, w and θ are necessarily positively correlated

so the cloudy regions are warmer, consistent with Ingersoll and Cuzzi's deduction.

The scale given in Table I for radiative instability is again the distance of the first node from the equator. This distance scale is characteristic of low-latitude disturbances in a motionless atmosphere (Lindzen 1967). The scale depends on the static stability, which is unknown, but we can estimate what value of the static stability would give the correct one for the banded structure. In particular, we know that the scale is given correctly, in order of magnitude, by Eq. (3). If we multiply this scale by two, so that it agrees with the observed one, and equate it to the scale given in Table I for the radiative instability, we find that the required static stability is

$$S \sim \frac{u^2}{\alpha g H^2}. \tag{17}$$

Substituting this value into Eq. (3), and assuming that $H \sim D$, we find that the corresponding value of the Richardson number is $Ri \sim 1$. Thus the radiative instability mechanism can account for the observed scale of the banded structure only under conditions such that inertial instability is also likely to occur. Since the two mechanisms generate very similar structures, they may well act simultaneously and reinforce each other. The relative efficiency of the two mechanisms may be compared by calculating their characteristic time scales, given in Table I. If we choose $Ri = \frac{1}{2}$, $\tau = 10^8$ sec (Gierasch and Goody 1969), $u = 100$ m sec^{-1}, $H = 20$ km, and evaluate f at 4° latitude, we find that the time scale for inertial instability is 4×10^4 sec and for radiative instability 10^6 sec. Apparently inertial instability would be a much more efficient mechanism for generating the banded structure. In fact, the very long radiative time scales in Jupiter's atmosphere mean that the time scales associated with the radiative instability are invariably much longer than those associated with the other instabilities listed in Table I, and therefore, it is doubtful whether it would be a dominant mechanism.

(c) Great Red Spot

Hide (1961, 1963) presented the first dynamical discussion of the Great Red Spot. He noted that the motions in the vicinity of the Spot resembled those seen in laboratory experiments with Taylor columns. These experiments show that, if a fluid is homogeneous and sufficiently rapidly rotating, even a shallow topographic feature will give rise to a disturbance in the flow pattern that propagates upward and appears at the top of the fluid (Taylor 1923). Such disturbances are sometimes referred to as "Taylor columns" and Hide suggested that the Great Red Spot was a manifestation of such a disturbance.

Hide's suggestion has stimulated a number of studies aimed at elucidating the properties of Taylor columns and the conditions under which they can occur. Recent experimental studies (Hide and Ibbetsen 1968) and theoreti-

cal studies (Ingersoll 1969) reinforce the conclusion that the observed flow patterns resemble those around a Taylor column. Calculations of the Rossby number in the vicinity of the Spot show that the atmosphere is sufficiently rapidly rotating for Taylor columns to occur (Hide 1963; Hess 1969). Stone and Baker (1968) criticized the Taylor column hypothesis on the grounds that the atmosphere's stratification and horizontal temperature gradients were not small enough for the atmosphere to be considered homogeneous. Recently Hogg (1973) analyzed the flow of a non-homogeneous fluid past an obstacle and found that Taylor columns can occur if

$$\frac{\alpha g S H^2}{f^2 L^2} \lesssim Ro\,. \tag{18}$$

This condition is plausible, since even if the atmosphere is isothermal, the Great Red Spot is so large that the left-hand side of Eq. (18) is still only ~ 0.03. In practice, it is likely that the atmosphere is nearly adiabatic, $S \ll \Gamma$, and then the condition is met, even though $Ro \sim 0.01$.

However, even if Eq. (18) is satisfied, Hogg's analysis does not demonstrate that Taylor columns can occur in a real atmosphere. He assumed that the flow was steady, yet his flow is baroclinically unstable. Since these instabilities transport heat, they will modify the flow pattern in his analysis. It is not clear how a Taylor column can be maintained under such conditions.

Other difficulties with the Taylor column hypothesis are the observation that the Great Red Spot does not have a fixed longitude (Peek 1958) and the likelihood that there is no solid surface (Hubbard 1973). To get around these difficulties, Streett (1969) suggested that the Spot was caused by a Taylor column attached to a mass of solid hydrogen floating in helium-rich liquid hydrogen deep in the atmosphere. Streett *et al.* (1971) attempted to analyze the dynamics of such a floating raft, but their analysis omitted Coriolis forces and, therefore, is not relevant to Jupiter.

Golitsyn (1970) suggested that the Spot was a long-lived eddy, i.e., that there need not be any immediate driving mechanism for the Spot. This idea receives some support from Ingersoll's (1973) analysis, showing that the equations of motion for large-scale flows on Jupiter contain free (i.e., unforced) solutions which resemble the flow patterns in the vicinity of the Spot. However, the idea that no forcing is present currently seems implausible since the radiative and dynamical time scales in Jupiter's atmosphere range from 10 years down to days (Gierasch and Goody 1969; Stone 1973*a*) and are considerably shorter than the time during which the Spot has been observed. Indeed, many changes in the circulations elsewhere in the atmosphere have been observed (Peek 1958). Ingersoll's (1973) analysis does lessen the attractiveness of the Taylor column hypothesis because it shows that one need not rely on a topographic feature to explain the observed flow patterns.

Another model of the Spot which treats it as a long-lived artifact has been presented by Maxworthy and Redekopp (1976). Their model is based on the

concept of "solitons" (Scott *et al.* 1973). These are finite amplitude solitary waves that persist without change in the absence of any dissipation, because dispersive effects are balanced by non-linear effects. Maxworthy and Redekopp found that solitons can exist in a stratified zonal flow that is incompressible, barotropic, and quasi-geostrophic, provided that

$$\frac{\pi^2 f^2 L^2}{\alpha g S D^2} \leqslant 1 . \tag{19}$$

L in their solution corresponds to about one third of the meridional extent of the Spot. Maxworthy and Redekopp found that the flow patterns accompanying these solitons closely resemble the flows observed in the vicinity of the Spot, including the flow observed when the Spot interacts with the South Tropical Disturbance. This latter interaction is not reproduced well by other theories of the Spot.

Eq. (19) in effect places a lower bound on the static stability which must be met if the soliton theory is to be viable. If we choose $\alpha = (130°\text{K})^{-1}$, $H =$ 20 km, $3L = 12000$ km, and evaluate f at 17° latitude, then Eq. (19) implies that $S \geqslant 20°/\text{km}$; i.e., that the temperature must be increasing with height by at least 18°/km in the vicinity of the Spot. This stability is so much greater than that at the 130°K level in any proposed model of the atmosphere, that the soliton model becomes implausible. It is worth noting that the soliton and Taylor column models require conditions [Eqs. (18) and (19)] which are mutually incompatible so long as $Ro \ll 1$. The fact that many different models can produce flow patterns resembling those around the Great Red Spot [i.e., Maxworthy and Redekopp's; Hide and Ibbetsen's (1968); Hogg's (1973); and Ingersoll's (1973)] suggests that such a resemblance *per se* does not provide strong support for any particular model.

Kuiper (1972) has suggested that the Great Red Spot is a region of organized cumulus convection driven by water vapor condensation. As pointed out in Sec. II, this energy source occurs down near the 300°K level and one would have to assume that the effect of the condensation is being felt in a region 10 or more vapor pressure scale-heights above the condensation level. In any case, the general idea that the Spot represents a disturbed region is plausible. In particular, Ingersoll (1973) has pointed out that the Spot appears to share the characteristics of the zones—i.e., cloudiness, anticyclonic vorticity and rising motions—and Prinn and Lewis (1975) have demonstrated that the red color of the Spot can be explained if the vertical mixing in the Spot is enhanced relative to the rest of the atmosphere. As yet, there seems to be no compelling theory for the nature of this disturbance.

(d) Non-symmetric Features

Two mechanisms have been proposed for explaining the many large-scale non-symmetric cloud features in the Jovian atmosphere. Stone (1967) has suggested that they are analogous to extra-tropical cyclones in the terrestrial

atmosphere, i.e., that they are caused by baroclinic instability. The discussion in Sec. III shows that it is very likely that horizontal temperature gradients occur in the visible cloud layers, at least on the scale of the belts and zones, if not on the planetary scale. Consequently, potential energy should be available for baroclinic perturbations to feed on. Thus it is quite possible that baroclinic instability occurs locally, even if it is not the dominant dynamical mode. The main uncertainty in postulating its existence in the Jovian atmosphere is again our ignorance of the static stability of the visible cloud layers and of the layers immediately below them.

The characteristic scale for baroclinic instability (see Table I) depends on the (unknown) value of Ri, but we can, nevertheless, place bounds on it by choosing extreme values. The range of Ri values for which baroclinic instability can occur is roughly $1 < Ri < 1000$ (see Fig. 2). If we choose $u \sim 10$ m sec^{-1}, then the bounds on the characteristic scale, at 30° latitude, are 150 km and 4000 km. This range includes the scales of many observed non-symmetric features. The corresponding range of time scales for baroclinic instability is 6 hours to 150 hours.

Ingersoll and Cuzzi (1969) have suggested that barotropic instability may be an important mechanism in the Jovian atmosphere. This instability draws its energy from the kinetic energy of the mean flow by means of horizontal eddy stresses and thereby tends to limit the horizontal shear in the mean flow. The most unstable modes are three-dimensional, so this mechanism is another possible source of the non-symmetric features seen in the Jovian atmosphere. The scale for this instability given in Table I again refers to the half-wavelength in the down-stream direction of the most unstable mode.

The barotropic instability criterion (see Table I) can be checked directly from observations. For example, if we use the mean distribution of u given by Chapman (1969), we find that d^2u/dy^2 exceeds β on the edges of the equatorial current and the north temperate current by a factor of ten. This excess is sufficient that uncertainties in interpreting the apparent horizontal shear as a real horizontal shear at a constant pressure level are unlikely to reverse the conclusion that barotropic instability should be occurring. In fact, the edges of the bands and currents often are perturbed, as, for example, in the Pioneer 10 photographs (Gehrels *et al.* 1974). If we choose 10 m sec^{-1} as a typical velocity, then the characteristic scale for barotropic instability is 5000 km. This scale is, in fact, about the scale of the larger perturbations observed. The corresponding characteristic time scale is 400 hours. Also the vortex-like features seen in the Pioneer 11 pictures (Swindell *et al.* 1975) resemble barotropic (shear) instabilities seen in laboratory experiments. Thus, barotropic instability appears to be a very plausible mechanism for generating at least some of the larger-scale non-symmetric features seen in the Jovian atmosphere.

V. SUMMARY

Theoretical calculations so far shed little light on the nature of Jupiter's circulations. About all one can say is that the regime in the visible cloud layers in low latitudes is likely to be an inertial instability or forced convection regime, with lapse rates very nearly adiabatic. Analytical models of these regimes and of finite amplitude rotating convection in the deep atmosphere are needed to further the deductive approach to Jovian meteorology. Measurements of the latitudinal variation of the internal heating are particularly important for developing realistic models.

On the other hand, it is possible to say something about the kinematics. The plausible assumption, that the zonal motions are in geostrophic balance and satisfy the thermal wind relation, enables one to deduce that the zones are regions of higher pressure, warmer temperatures, rising motions and enhanced cloudiness, while the belts are regions of lower pressure, cooler temperatures, sinking motions and relatively cloud-free. These temperature differences imply that baroclinic energy sources are present. The strong shear at the edges of some belts indicate that barotropic instability should occur, and this could account for at least some of the larger-scale non-symmetric features of the belts. To evaluate different speculations for the causes of the banded structure and other non-symmetric features, it would be valuable to have measurements of meridional velocities, measurements of the lapse rates, and static stability in both the cloud layers and the layers immediately below, and to have high-resolution visual observations capable of resolving small-scale convection.

REFERENCES

Aumann, H. H.; Gillespie, C. M., Jr.; and Low, F. J. 1969. The internal powers and effective temperatures of Jupiter and Saturn. *Astrophys. J.* 157:L69–L72.

Barcilon, A., and Gierasch, P. 1970. A moist, Hadley cell model for Jupiter's cloud bands. *J. Atmos. Sci.* 27:550–560.

Businger, J. A.; Wyngaard, J. C.; Izumi, Y.; and Bradley, E. F. 1971. Flux-profile relationships in the atmospheric surface layer. *J. Atmos. Sci.* 28:181–189.

Busse, F. H. 1970*a*. Thermal instabilities in rapidly rotating systems. *J. Fluid. Mech.* 44:441–460.

———. 1970*b*. Differential rotation in stellar convection zones. *Astrophys. J.* 159:629–639.

———. 1976. A simple model of convection in the Jovian atmosphere. *Icarus* (special Jupiter issue). In press.

Chandrasekhar, S. 1961. *Hydrodynamic and hydromagnetic stability*. Oxford: Clarendon Press.

Chapman, C. R. 1969. Jupiter's zonal winds: variation with latitude. *J. Atmos. Sci.* 26:986–990.

Chase, S. C.; Ruiz, R. D.; Münch, G.; Neugebauer, G.; Schroeder, M.; and Trafton, L. M. 1974. Pioneer 10 infrared radiometer experiment: preliminary results. *Science* 183:315–317.

Divine, T. N. 1971. The planet Jupiter. NASA SP-8069. Washington, D.C.: Government Printing Office.

Drazin, P. G., and Howard, L. N. 1966. Hydrodynamic stability of parallel flow of inviscid fluid. *Advanc. Appl. Mech.* 9:1–89.

Gehrels, T. 1974. The convectively unstable atmosphere of Jupiter. *J. Geophys. Res.* 79: 4305–4307.

Gehrels, T.; Coffeen, D.; Tomasko, M.; Doose, L.; Swindell, W.; Castillo, N.; Kendall, J.; Clements, A.; Hämeen-Anttila, J.; KenKnight, C.; Blenman, C.; Baker, R.; Best, G.; and Baker, L. 1974. The imaging photopolarimeter experiment on Pioneer 10. *Science* 183: 318–320.

Gierasch, P. J. 1970. The fourth Arizona Conference on planetary atmospheres: motions of planetary atmospheres. *Earth Extraterr. Sci.* 1:171–184.

———. 1973. Jupiter's cloud bands. *Icarus* 19:482–494.

Gierasch, P., and Goody, R. M. 1969. Radiative time constants in the atmosphere of Jupiter. *J. Atmos. Sci.* 26:979–980.

Gierasch, P.; Goody, R.; and Stone, P. 1970. The energy balance of planetary atmospheres. *Geophys. Fluid Dyn.* 1:1–18.

Gierasch, P. J.; Ingersoll, A. P.; and Williams, R. T. 1973. Radiative instability of a cloudy planetary atmosphere. *Icarus* 19:473–481.

Gierasch, P. J., and Stone, P. H. 1968. A mechanism for Jupiter's equatorial acceleration. *J. Atmos. Sci.* 25:1169–1170.

———. 1972. Reply. *J. Atmos. Sci.* 29:1008.

Golitsyn, G. S. 1970. A similarity approach to the general circulation of planetary atmospheres. *Icarus* 13:1–24.

Goody, R. 1969. Motions of planetary atmospheres. *Annual Rev. Astron. Astrophys.* 7:303–352.

Hadlock, R. K.; Na, J. Y.; and Stone, P. H. 1972. Direct thermal verification of symmetric baroclinic instability. *J. Atmos. Sci.* 29:1391–1393.

Hartmann, W. K. 1974. Martian and terrestrial paleoclimatology: relevance of solar variability. *Icarus* 22:301–311.

Hess, S. L. 1969. Vorticity, Rossby number, and geostrophy in the atmosphere of Jupiter. *Icarus* 11:218–219.

Hess, S. L., and Panofsky, H. A. 1951. The atmospheres of the other planets. *Compendium of Meteorology*, pp. 391–400. Boston: American Meteorological Society.

Hide, R. 1961. Origin of Jupiter's Great Red Spot. *Nature* 190:895.

———. 1963. On the hydrodynamics of Jupiter's atmosphere. *Mém. Soc. Roy. Sci. Liège (Sér. V)* VII:481–505.

———. 1966. On the circulation of the atmospheres of Jupiter and Saturn. *Planet. Space Sci.* 14:669–675.

———. 1969. Dynamics of the atmospheres of the major planets with an appendix on the viscous boundary layer at the rigid bounding surface of an electrically-conducting rotating fluid in the presence of a magnetic field. *J. Atmos. Sci.* 26:841–853.

———. 1970. Equatorial jets in planetary atmospheres. *Nature* 225:254.

Hide, R., and Ibbetsen, A. 1968. On slow transverse flow past obstacles in a rapidly rotating fluid. *J. Fluid Mech.* 32:251–272.

Hogan, J.; Rasool, S. I.; and Encrenaz, T. 1969. The thermal structure of the Jovian atmosphere. *J. Atmos. Sci.* 26:898–905.

Hogg, N. G. 1973. On the stratified Taylor column. *J. Fluid Mech.* 58:517–537.

Holton, J. R. 1972. *An introduction to dynamic meteorology*. New York: Academic Press.

Holton, J. R., and Lindzen, R. S. 1972. An updated theory for the quasi-biennial cycle of the tropical atmosphere. *J. Atmos. Sci.* 29:1076–1080.

Hubbard, W. B. 1973. The significance of atmospheric measurements for interior models of the major planets. *Space Sci. Rev.* 14:424–432.

Ingersoll, A. P. 1969. Inertial Taylor columns and Jupiter's Great Red Spot. *J. Atmos. Sci.* 26:744–752.

———. 1973. Jupiter's Great Red Spot: a free atmospheric vortex? *Science* 182:1346–1348.

Ingersoll, A. P., and Cuzzi, J. N. 1969. Dynamics of Jupiter's cloud bands. *J. Atmos. Sci.* 26: 981–985.

Ingersoll, A. P. 1976. Pioneer 10 and 11 observations and the dynamics of Jupiter's atmosphere. *Icarus* (special Jupiter issue). In press.

Kliore, A. J.; Fjeldbo, G.; Seidel, B. L.; Sykes, M. J.; and Woiceshyn, P. 1973. S-band radio occultation measurements of the atmosphere and topography of Mars with Mariner 9: extended mission coverage of polar and intermediate latitudes. *J. Geophys. Res.* 78:4331–4351.

Kuiper, G. P. 1972. Lunar and Planetary Laboratory studies of Jupiter—II. *Sky and Telescope* 43:75–81.

Kuo, H. L. 1949. Dynamic instability of two-dimensional non-divergent flow in a barotropic atmosphere. *J. Meteor.* 6:105–122.

Lewis, J. S. 1969. The clouds of Jupiter and the NH_3-H_2O and NH_3-H_2S systems. *Icarus* 10: 365–378.

Lindzen, R. D. 1967. Planetary waves on beta-planes. *Mon. Wea. Rev.* 95:441–451.

Maxworthy, T. 1972. Comments on a mechanism for Jupiter's equatorial acceleration. *J. Atmos. Sci.* 29:1007–1008.

———. 1973. A review of Jovian atmospheric dynamics. *Planet. Space Sci.* 21:623–641.

———. 1975. A wave driven model of the Jovian equatorial jet. *Planet. Space Sci.* In press.

Maxworthy, T. and Redekopp, L. G. 1976. A solitary wave theory of the Great Red Spot and other observed features in the Jovian atmosphere. *Icarus* (special Jupiter issue). In press.

McIntyre, M. E. 1970. Diffusive destabilization of the baroclinic circular vortex. *Geophys. Fluid Dyn.* 1:19–57.

———. 1972. Baroclinic instability of an idealized model of the polar night jet. *Quart. J. Roy. Meteor. Soc.* 98:165–174.

Newburn, R. L., Jr., and Gulkis, S. 1973. A survey of the outer planets Jupiter, Saturn, Uranus, Neptune, Pluto, and their satellites. *Space Sci. Rev.* 3:179–271.

Ogura, Y. and Cho, H. R. 1973. Diagnostic determination of cumulus cloud populations from observed large-scale variables. *J. Atmos. Sci.* 30:1276–1286.

Peek, B. M. 1958. *The Planet Jupiter.* London: Faber and Faber.

Phillips, N. A. 1951. A simple three-dimensional model for the study of large-scale extratropical flow patterns. *J. Meteor.* 8:381–394.

Priestly, C. H. B. 1959. *Turbulent transfer in the lower atmosphere.* Chicago: Univ. of Chicago Press.

Prinn, R. G., and Lewis, J. S. 1975. Phosphine on Jupiter and implications for the Great Red Spot. *Science.* In press.

Reese, E. J., and Smith, B. A. 1968. Evidence of vorticity in the Great Red Spot of Jupiter. *Icarus* 9:474–486.

Roberts, P. H. 1968. On the thermal instability of a rotating fluid sphere containing heat sources. *Phil. Trans. Roy. Soc. London* A263:93–117.

Sagan, C.; Toon, O.; and Gierasch, P. 1973. Climatic change on Mars. *Science* 181:1045–1049.

Scott, A. G.; Chu, F. Y. F.; and McLaughlin, D. W. 1973. The soliton: a new concept in applied science. *Proc. IEEE* 61:1443–1483.

Slipher, E. C.; Hess, S. L.; Blackadar, A. K.; Gidas, H. L.; Shapiro, R.; Lorenz, E. N.; Gifford, F. A.; Mintz, Y.; and Johnson, H. L. 1952. The study of planetary atmospheres. *Lowell Obs. Final Report,* Contract No. AF19 122–162.

Spiegel, E. A. 1971. Convection in stars: I. Basic Boussinesq convection. *Ann. Rev. Astron. Astrophys.* 9:323–352.

Stone, P. H. 1966. On non-geostrophic baroclinic stability. *J. Atmos. Sci.* 23:390–400.

———. 1967. An application of baroclinic stability theory to the dynamics of the Jovian atmosphere. *J. Atmos. Sci.* 24:642–652.

Stone, P. H. 1970. On non-geostrophic baroclinic stability: Part II. *J. Atmos. Sci.* 27:721–726.
———. 1971. The symmetric baroclinic instability of an equatorial current. *Geophys. Fluid Dyn.* 2:147–164.
———. 1972*a*. On non-geostrophic baroclinic stability: Part III. The momentum and heat transports. *J. Atmos. Sci.* 29:419–426.
———. 1972*b*. A simplified radiative-dynamical model for the static stability of rotating atmospheres. *J. Atmos. Sci.* 29:405–418.
———. 1973*a*. The dynamics of the atmospheres of the major planets. *Space Sci. Rev.* 14:444–459.
———. 1973*b*. The effect of large-scale eddies on climatic change. *J. Atmos. Sci.* 30:521–529.
———. 1974. On Jupiter's rate of rotation. *J. Atmos. Sci.* 31:1471–1472.
Stone, P. H., and Baker, D. J., Jr. 1968. Concerning the existence of Taylor columns in atmospheres. *Quart. J. Roy. Meteor. Soc.* 94:576–580.
Stone, P. H.; Hess, S.; Hadlock, R.; and Ray, P. 1969. Preliminary results of experiments with symmetric baroclinic instabilities. *J. Atmos. Sci.* 26:991–996.
Streett, W. B. 1969. Phase equilibria in planetary atmospheres. *J. Atmos. Sci.* 26:924–931.
Streett, W. B.; Ringermacher, H. I.; and Veronis, G. 1971. On the structure and motions of Jupiter's Red Spot. *Icarus* 14:319–342.
Swindell, W.; Doose, L. R.; Tomasko, M.; and Fountain, J. 1975. The Pioneer 11 images of Jupiter. *Bull. Amer. Astron. Soc.* 7:378.
Taylor, G. I. 1923. Experiments on the motion of solid bodies in rotating fluids. *Proc. Roy. Soc. (London)* A104:213–218.
Trafton, L. M. 1967. Model atmospheres of the major planets. *Astrophys. J.* 147:765–781.
Trafton, L. M., and Stone, P. H. 1974. Radiative-dynamical equilibrium states for Jupiter. *Astrophys. J.* 188:649–655.
Walton, I. C. 1975. The viscous non-linear symmetric baroclinic instability of a zonal shear flow. *J. Fluid Mech.* 68:757–768.
Weidenschilling, S. J., and Lewis, J. S. 1973. Atmospheric and cloud structures of the Jovian planets. *Icarus* 20:465–476.
Westphal, J. A. 1971. Observations of Jupiter's cloud structure near 8.5 μ. *Planetary atmospheres.* (C. Sagan, T. C. Owen, H. J. Smith, eds.) pp. 359–362. Dordrecht, Holland: D. Reidel Publ. Co.
Whitehead, J. A., Jr. 1975. Mean flow generated by circulation on a β-plane: an analogy with the moving flame experiment. *Tellus* 26. In press.
Williams, G. P., and Robinson, J. B. 1973. Dynamics of a convectively unstable atmosphere: Jupiter? *J. Atmos. Sci.* 30:684–717.